

Evolução na Ciência e Engenharia de Materiais

Henrique Ajuz Holzmann
(Organizador)



Atena
Editora

Ano 2020

Evolução na Ciência e Engenharia de Materiais

Henrique Ajuz Holzmann
(Organizador)



Atena
Editora

Ano 2020

2020 by Atena Editora

Copyright © Atena Editora

Copyright do Texto © 2020 Os autores

Copyright da Edição © 2020 Atena Editora

Editora Chefe: Profª Drª Antonella Carvalho de Oliveira

Diagramação: Karine de Lima

Edição de Arte: Lorena Prestes

Revisão: Os Autores



Todo o conteúdo deste livro está licenciado sob uma Licença de Atribuição *Creative Commons*. Atribuição 4.0 Internacional (CC BY 4.0).

O conteúdo dos artigos e seus dados em sua forma, correção e confiabilidade são de responsabilidade exclusiva dos autores. Permitido o download da obra e o compartilhamento desde que sejam atribuídos créditos aos autores, mas sem a possibilidade de alterá-la de nenhuma forma ou utilizá-la para fins comerciais.

Conselho Editorial

Ciências Humanas e Sociais Aplicadas

Profª Drª Adriana Demite Stephani – Universidade Federal do Tocantins
Prof. Dr. Álvaro Augusto de Borba Barreto – Universidade Federal de Pelotas
Prof. Dr. Alexandre Jose Schumacher – Instituto Federal de Educação, Ciência e Tecnologia de Mato Grosso
Prof. Dr. Antonio Carlos Frasson – Universidade Tecnológica Federal do Paraná
Prof. Dr. Antonio Gasparetto Júnior – Instituto Federal do Sudeste de Minas Gerais
Prof. Dr. Antonio Isidro-Filho – Universidade de Brasília
Prof. Dr. Carlos Antonio de Souza Moraes – Universidade Federal Fluminense
Prof. Dr. Constantino Ribeiro de Oliveira Junior – Universidade Estadual de Ponta Grossa
Profª Drª Cristina Gaio – Universidade de Lisboa
Profª Drª Denise Rocha – Universidade Federal do Ceará
Prof. Dr. Deyvison de Lima Oliveira – Universidade Federal de Rondônia
Prof. Dr. Edvaldo Antunes de Farias – Universidade Estácio de Sá
Prof. Dr. Eloi Martins Senhora – Universidade Federal de Roraima
Prof. Dr. Fabiano Tadeu Grazioli – Universidade Regional Integrada do Alto Uruguai e das Missões
Prof. Dr. Gilmei Fleck – Universidade Estadual do Oeste do Paraná
Profª Drª Ivone Goulart Lopes – Istituto Internazionale delle Figlie di Maria Ausiliatrice
Prof. Dr. Julio Candido de Meirelles Junior – Universidade Federal Fluminense
Profª Drª Keyla Christina Almeida Portela – Instituto Federal de Educação, Ciência e Tecnologia de Mato Grosso
Profª Drª Lina Maria Gonçalves – Universidade Federal do Tocantins
Profª Drª Natiéli Piovesan – Instituto Federal do Rio Grande do Norte
Prof. Dr. Marcelo Pereira da Silva – Universidade Federal do Maranhão
Profª Drª Miranilde Oliveira Neves – Instituto de Educação, Ciência e Tecnologia do Pará
Profª Drª Paola Andressa Scortegagna – Universidade Estadual de Ponta Grossa
Profª Drª Rita de Cássia da Silva Oliveira – Universidade Estadual de Ponta Grossa
Profª Drª Sandra Regina Gardacho Pietrobon – Universidade Estadual do Centro-Oeste
Profª Drª Sheila Marta Carregosa Rocha – Universidade do Estado da Bahia
Prof. Dr. Rui Maia Diamantino – Universidade Salvador
Prof. Dr. Urandi João Rodrigues Junior – Universidade Federal do Oeste do Pará
Profª Drª Vanessa Bordin Viera – Universidade Federal de Campina Grande
Prof. Dr. William Cleber Domingues Silva – Universidade Federal Rural do Rio de Janeiro
Prof. Dr. Willian Douglas Guilherme – Universidade Federal do Tocantins

Ciências Agrárias e Multidisciplinar

Prof. Dr. Alexandre Igor Azevedo Pereira – Instituto Federal Goiano
Prof. Dr. Antonio Pasqualetto – Pontifícia Universidade Católica de Goiás
Profª Drª Daiane Garabeli Trojan – Universidade Norte do Paraná

Profª Drª Diocléa Almeida Seabra Silva – Universidade Federal Rural da Amazônia
Prof. Dr. Écio Souza Diniz – Universidade Federal de Viçosa
Prof. Dr. Fábio Steiner – Universidade Estadual de Mato Grosso do Sul
Prof. Dr. Fágner Cavalcante Patrocínio dos Santos – Universidade Federal do Ceará
Profª Drª Girlene Santos de Souza – Universidade Federal do Recôncavo da Bahia
Prof. Dr. Júlio César Ribeiro – Universidade Federal Rural do Rio de Janeiro
Profª Drª Lina Raquel Santos Araújo – Universidade Estadual do Ceará
Prof. Dr. Pedro Manuel Villa – Universidade Federal de Viçosa
Profª Drª Raissa Rachel Salustriano da Silva Matos – Universidade Federal do Maranhão
Prof. Dr. Ronilson Freitas de Souza – Universidade do Estado do Pará
Profª Drª Talita de Santos Matos – Universidade Federal Rural do Rio de Janeiro
Prof. Dr. Tiago da Silva Teófilo – Universidade Federal Rural do Semi-Árido
Prof. Dr. Valdemar Antonio Paffaro Junior – Universidade Federal de Alfenas

Ciências Biológicas e da Saúde

Prof. Dr. André Ribeiro da Silva – Universidade de Brasília
Profª Drª Anelise Levay Murari – Universidade Federal de Pelotas
Prof. Dr. Benedito Rodrigues da Silva Neto – Universidade Federal de Goiás
Prof. Dr. Edson da Silva – Universidade Federal dos Vales do Jequitinhonha e Mucuri
Profª Drª Eleuza Rodrigues Machado – Faculdade Anhanguera de Brasília
Profª Drª Elane Schwinden Prudêncio – Universidade Federal de Santa Catarina
Prof. Dr. Ferlando Lima Santos – Universidade Federal do Recôncavo da Bahia
Prof. Dr. Gianfábio Pimentel Franco – Universidade Federal de Santa Maria
Prof. Dr. Igor Luiz Vieira de Lima Santos – Universidade Federal de Campina Grande
Prof. Dr. José Max Barbosa de Oliveira Junior – Universidade Federal do Oeste do Pará
Profª Drª Magnólia de Araújo Campos – Universidade Federal de Campina Grande
Profª Drª Mylena Andréa Oliveira Torres – Universidade Ceuma
Profª Drª Natiéli Piovesan – Instituto Federaci do Rio Grande do Norte
Prof. Dr. Paulo Inada – Universidade Estadual de Maringá
Profª Drª Vanessa Lima Gonçalves – Universidade Estadual de Ponta Grossa
Profª Drª Vanessa Bordin Viera – Universidade Federal de Campina Grande

Ciências Exatas e da Terra e Engenharias

Prof. Dr. Adélio Alcino Sampaio Castro Machado – Universidade do Porto
Prof. Dr. Alexandre Leite dos Santos Silva – Universidade Federal do Piauí
Prof. Dr. Carlos Eduardo Sanches de Andrade – Universidade Federal de Goiás
Profª Drª Carmen Lúcia Voigt – Universidade Norte do Paraná
Prof. Dr. Eloi Rufato Junior – Universidade Tecnológica Federal do Paraná
Prof. Dr. Fabrício Menezes Ramos – Instituto Federal do Pará
Prof. Dr. Juliano Carlo Rufino de Freitas – Universidade Federal de Campina Grande
Prof. Dr. Marcelo Marques – Universidade Estadual de Maringá
Profª Drª Neiva Maria de Almeida – Universidade Federal da Paraíba
Profª Drª Natiéli Piovesan – Instituto Federal do Rio Grande do Norte
Prof. Dr. Takeshy Tachizawa – Faculdade de Campo Limpo Paulista

Conselho Técnico Científico

Prof. Msc. Abrãao Carvalho Nogueira – Universidade Federal do Espírito Santo
Prof. Msc. Adalberto Zorzo – Centro Estadual de Educação Tecnológica Paula Souza
Prof. Dr. Adailson Wagner Sousa de Vasconcelos – Ordem dos Advogados do Brasil/Seccional Paraíba
Prof. Msc. André Flávio Gonçalves Silva – Universidade Federal do Maranhão
Profª Drª Andreza Lopes – Instituto de Pesquisa e Desenvolvimento Acadêmico
Profª Msc. Bianca Camargo Martins – UniCesumar
Prof. Msc. Carlos Antônio dos Santos – Universidade Federal Rural do Rio de Janeiro
Prof. Msc. Cláudia de Araújo Marques – Faculdade de Música do Espírito Santo
Prof. Msc. Daniel da Silva Miranda – Universidade Federal do Pará
Profª Msc. Dayane de Melo Barros – Universidade Federal de Pernambuco

Prof. Dr. Edwaldo Costa – Marinha do Brasil
 Prof. Msc. Eliel Constantino da Silva – Universidade Estadual Paulista Júlio de Mesquita
 Prof. Msc. Gevair Campos – Instituto Mineiro de Agropecuária
 Prof. Msc. Guilherme Renato Gomes – Universidade Norte do Paraná
 Prof^a Msc. Jaqueline Oliveira Rezende – Universidade Federal de Uberlândia
 Prof. Msc. José Messias Ribeiro Júnior – Instituto Federal de Educação Tecnológica de Pernambuco
 Prof. Msc. Leonardo Tullio – Universidade Estadual de Ponta Grossa
 Prof^a Msc. Lilian Coelho de Freitas – Instituto Federal do Pará
 Prof^a Msc. Liliani Aparecida Sereno Fontes de Medeiros – Consórcio CEDERJ
 Prof^a Dr^a Lívia do Carmo Silva – Universidade Federal de Goiás
 Prof. Msc. Luis Henrique Almeida Castro – Universidade Federal da Grande Dourados
 Prof. Msc. Luan Vinicius Bernardelli – Universidade Estadual de Maringá
 Prof. Msc. Rafael Henrique Silva – Hospital Universitário da Universidade Federal da Grande Dourados
 Prof^a Msc. Renata Luciane Polsaque Young Blood – UniSecal
 Prof^a Msc. Solange Aparecida de Souza Monteiro – Instituto Federal de São Paulo
 Prof. Dr. Welleson Feitosa Gazel – Universidade Paulista

**Dados Internacionais de Catalogação na Publicação (CIP)
(eDOC BRASIL, Belo Horizonte/MG)**

E93 Evolução na ciência e engenharia de materiais [recurso eletrônico] /
 Organizador Henrique Ajuz Holzmann. – Ponta Grossa, PR:
 Atena Editora, 2020.

Formato: PDF
 Requisitos de sistema: Adobe Acrobat Reader
 Modo de acesso: World Wide Web
 Inclui bibliografia
 ISBN 978-85-7247-921-9
 DOI 10.22533/at.ed.219201601

1. Engenharia de materiais – Pesquisa – Brasil. I. Holzmann,
 Henrique Ajuz.

CDD 620.11

Elaborado por Maurício Amormino Júnior – CRB6/2422

Atena Editora
 Ponta Grossa – Paraná - Brasil
www.atenaeditora.com.br
contato@atenaeditora.com.br

APRESENTAÇÃO

A engenharia de materiais, se tornou um dos grandes pilares da revolução técnica industrial, devido a necessidade de desenvolvimento de novos materiais, que apresentem melhores características e propriedades físico-químicas. Grandes empresas e centros de pesquisa investem maciçamente em setores de P&D a fim de tornarem seus produtos e suas tecnologias mais competitivas.

Destaca-se que a área de material compreende três grandes grupos, a dos metais, das cerâmicas e dos polímeros, sendo que cada um deles tem sua importância na geração de tecnologia e no desenvolvimento dos produtos. Aliar os conhecimentos pré-existentes com novas tecnologias é um dos grandes desafios da nova engenharia.

Neste livro são explorados trabalhos teóricos e práticos, relacionados as áreas de materiais, dando um panorama dos assuntos em pesquisa atualmente. Apresenta capítulos relacionados ao desenvolvimento de novos materiais, com aplicações nos mais diversos ramos da ciência, bem como assuntos relacionados a melhoria em processos e produtos já existentes, buscando uma melhoria e a redução dos custos.

De abordagem objetiva, a obra se mostra de grande relevância para graduandos, alunos de pós-graduação, docentes e profissionais, apresentando temáticas e metodologias diversificadas, em situações reais.

Boa leitura!

Henrique Ajuz Holzmann

SUMÁRIO

CAPÍTULO 1	1
INFLUÊNCIA DO ESPAÇAMENTO DE FIBRAS VEGETAIS NA RESISTÊNCIA À TRAÇÃO E MORFOLOGIA DA FRATURA DE COMPÓSITOS COM FIBRAS CONTÍNUAS E ALINHADAS	
Fábio Santos de Sousa Edwillson Gonçalves de Oliveira Filho Luciano Monteiro Almeida Roberto Tetsuo Fujiyama	
DOI 10.22533/at.ed.2192016011	
CAPÍTULO 2	10
COMPÓSITOS POLIMÉRICOS HÍBRIDOS COM FIBRAS NATURAIS E SINTÉTICAS CONTÍNUAS E ALINHADAS	
Luciano Monteiro Almeida César Tadeu Nasser Medeiros Branco Douglas Santos Silva Edwillson Gonçalves de Oliveira Filho Roberto Tetsuo Fujiyama	
DOI 10.22533/at.ed.2192016012	
CAPÍTULO 3	23
CARACTERIZAÇÃO DE NANOFILTRO REDUTOR DE SULFETO DE HIDROGÊNIO E UMIDADE DO BIOGÁS	
Mateus Sousa Pinheiro Gabrielle Dias Coelho Maria del Pilar Hidalgo Falla	
DOI 10.22533/at.ed.2192016013	
CAPÍTULO 4	36
DESCRIÇÃO TERMODINÂMICA DE MICRODOMÍNIOS DENTRO DE PICHE MESOFÁSICO PRECURSOR PARA FIBRAS DE CARBONO	
Caio Cesar Ferreira Florindo Adalberto Bono Maurizio Sacchi Bassi	
DOI 10.22533/at.ed.2192016014	
CAPÍTULO 5	51
NANOBIOSENSOR ELETROQUÍMICO BASEADO EM APTAMERO PARA DETECÇÃO DE OCRATOXINA A EM CAFÉ TORRADO	
Maurília Palmeira da Costa Itala Gabriela Tavares Lima Idjane Silva de Oliveira Cesar Augusto Souza de Andrade Maria Danielly Lima de Oliveira	
DOI 10.22533/at.ed.2192016015	

CAPÍTULO 6 63

DETECÇÃO ESPECÍFICA DE SCHISTOSOMA MANSONI EM LCR USANDO UM BIOSSENSOR ELETROQUÍMICO DE DNA BASEADO EM NANOPARTICULAS DE OURO E MERCAPTOSILANO

Giselle Soares dos Santos
César Augusto Sousa de Andrade
Fábio Lopes de Melo
Maria Danielly Lima de Oliveira

DOI 10.22533/at.ed.2192016016

CAPÍTULO 7 73

PRODUÇÃO DE NANOMATERIAIS BIOMIMÉTICOS A PARTIR DE UM NOVO SISTEMA DE *ELECTROSPINNING* PARA ENGENHARIA DE TECIDOS DOS MENISCOS DO JOELHO

Thiago Domingues Stocco
Anderson de Oliveira Lobo

DOI 10.22533/at.ed.2192016017

CAPÍTULO 8 87

PLATAFORMA NANOSTRUTURADA BASEADA EM APTÂMERO PARA DETECÇÃO DE OCRATOXINA A

Maurília Palmeira da Costa
Ítala Gabriela Tavares Lima
Idjane Silva de Oliveira
Cesar Augusto Souza de Andrade
Maria Danielly Lima de Oliveira

DOI 10.22533/at.ed.2192016018

CAPÍTULO 9 96

CARACTERIZAÇÃO DE NANOCOMPÓSITOS PLA/ZNO POR REOLOGIA E NMR NO DOMÍNIO DO TEMPO

Amanda Ramos Aragão Melo
José Carlos Dutra Filho
Maria Inês Bruno Tavares

DOI 10.22533/at.ed.2192016019

CAPÍTULO 10 108

INFLUÊNCIA DA SUBSTITUIÇÃO DE CÁLCIO E BÁRIO EM COMPOSIÇÕES DE PEROVSKITAS $TR_{(1-x)}M_xO_3$ (TR= PR, GD), (M = CA, BA) (X= 0,2) NA ATIVIDADE CATALÍTICA

Cássia Carla de Carvalho
Anderson Costa Marques
Symone Leandro de Castro
Davidson Nunes de Oliveira
Filipe Martel de Magalhães Borges
Alexandre de Sousa Campos

DOI 10.22533/at.ed.21920160110

CAPÍTULO 11 119

CERÂMICAS AVANÇADAS: PRODUÇÃO DE NANOESTRUTURAS DE ÓXIDOS TERRA RARA-NÍQUEL

Bruna Niccoli Ramirez
Márcia Tsuyama Escote

DOI 10.22533/at.ed.21920160111

CAPÍTULO 12 133

INSERÇÃO DE ESCÂNDIO E FÓSFORO NO SEMICONDUTOR DE DIÓXIDO DE TITÂNIO PARA APLICAÇÃO EM FOTOCATÁLISE

Eduardo Felipe De Carli
Eliane Kujat Fischer
Natali Amarante da Cruz
Alberto Adriano Cavalheiro

DOI 10.22533/at.ed.21920160112

CAPÍTULO 13 146

INDUTORES DE RÁDIO FREQUÊNCIA EXTERNOS COM ALTOS FATORES DE QUALIDADE USANDO OURO, SU8 E ALUMINA

Lucas Martins Miranda de Almeida
Alexandre da Silva Nascimento
Richard Alexandrino de Macedo
Angélica dos Anjos Ayala

DOI 10.22533/at.ed.21920160113

CAPÍTULO 14 153

INCLUSÃO DE NANOPARTÍCULAS DE $3Y-ZrO_2$ EM MATRIZ DE $\alpha-AL_2O_3$ PARA CONFEÇÃO DE INSERTO CERÂMICO

Miguel Adriano Inácio
José Victor Candido de Souza
Maria do Carmo de Andrade Nono
Sergio Luiz Mineiro
Daniel Alessander Nono

DOI 10.22533/at.ed.21920160114

CAPÍTULO 15 160

OPTICAL AND ELECTROCHEMICAL PROPERTIES IN CDSE/CDTE AND CDSE/CDTE NANOCRYSTALS PREPARED BY AQUEOUS SYNTHESIS

Raul Fernando Cuevas Rojas
Miguel Angel González Balanta
Silvio José Prado
Pablo Henrique Menezes
Lauro Antonio Pradela Filho
Victor Ciro Solano Reynoso

DOI 10.22533/at.ed.21920160115

CAPÍTULO 16 170

PRODUCTION OF ALKALINE PHOSPHATASE BY DENTAL PULP STEM CELLS IN INTERFACE WITH PLASMA MODIFIED TITANIUM

Keylla Dayanne Coelho Marinho de Melo
Laís Albuquerque Vasconcelos
Clodomiro Alves Junior
Jussier Oliveira Vitoriano
Hugo Alexandre de Oliveira Rocha
Moacir Fernandes de Queiroz Neto
José Sandro Pereira da Silva

DOI 10.22533/at.ed.21920160116

CAPÍTULO 17 187

SÍNTESE HIDROTÉRMICA ASSISTIDA POR MICRO-ONDAS DE ALUMINA TRI-HIDRATADA

Ricardo Ritter de Souza Barnasky
Cristiane Wienke Raubach Ratmann
Marciel Gaier
Mário Lúcio Moreira
Sergio da Silva Cava

DOI 10.22533/at.ed.21920160117

CAPÍTULO 18 201

MODIFICAÇÃO QUÍMICA DA LIGA DE ALUMÍNIO 5052 PARA OBTENÇÃO DE SUPERFÍCIES SUPER-HIDROFÓBICAS

Rafael Gleymir Casanova da Silva
Maria Isabel Collasius Malta
Severino Leopoldino Urtiga Filho
Sara Horácio de Oliveira
Magda Rosângela Santos Vieira

DOI 10.22533/at.ed.21920160118

CAPÍTULO 19 207

INFLUENCE OF THE ALUMINA ADDITION IN THE WEAR RESISTANCE OF THE SINTERED AISI 52100 STEEL

Bruna Horta Bastos Kuffner
Gilbert Silva
Carlos Alberto Rodrigues
Geovani Rodrigues

DOI 10.22533/at.ed.21920160119

CAPÍTULO 20 212

IMPROVEMENT OF TITANIUM SURFACE WITH PLASMA NITRIDING TREATMENT

Laís Albuquerque Vasconcelos
Keylla Dayanne Coelho Marinho de Melo
Clodomiro Alves Junior
Jussier Oliveira Vitoriano
Hugo Alexandre de Oliveira Rocha
Moacir Fernandes de Queiroz Neto
José Sandro Pereira da Silva

DOI 10.22533/at.ed.21920160120

CAPÍTULO 21 226

AValiação de termofosfatos de alumínio com a adição de escória siderúrgica

Maria Sílvia Camarão de Sousa
Oscar Jesus Choque Fernandez
Edilson Carvalho Brasil
Marcondes Lima da Costa
Érika Raiol Pinheiro
Marlo Oliveira Costa

DOI 10.22533/at.ed.21920160121

CAPÍTULO 22 236

CARACTERIZAÇÃO DA LAMA DE ALTO-FORNO DE UMA SIDERÚRGICA INTEGRADA DO SUDESTE DO PARÁ

Wellington Bruno Silva de Jesus
Alacid do Socorro Siqueira Neves
Emanuel Negrão Macêdo
José Antônio da Silva Souza
Luiz Felipe Silva Pereira
Roseane de Lima Silva
Verônica Scarpini Cândido
Antonio Lourenço da Costa Neto
Raimunda Figueiredo da Silva Maia
Daniel José Lima de Sousa

DOI 10.22533/at.ed.21920160122

CAPÍTULO 23 242

MÉTODO EQUACIONADO PARA PREVISÃO DO TEMPO DE REMOAGEM DE MINÉRIO DE FERRO

Simone Silva Neves
Filipe Mattos Gonçalves
Júnia Soares Alexandrino
Telma Ellen Drumond Ferreira

DOI 10.22533/at.ed.21920160123

SOBRE O ORGANIZADOR..... 254

ÍNDICE REMISSIVO 255

PRODUCTION OF ALKALINE PHOSPHATASE BY DENTAL PULP STEM CELLS IN INTERFACE WITH PLASMA MODIFIED TITANIUM

Data de aceite: 08/01/2020

Keylla Dayanne Coelho Marinho de Melo

MSc, Pos-graduating program in Health Science,
Universidade Federal do Rio Grande do
Norte Natal-RN

Laís Albuquerque Vasconcelos

DDS, Department of Dentistry, Universidade
Federal do Rio Grande do Norte Natal-RN

Clodomiro Alves Junior

PhD, Department of Materials Engineering,
Universidade Federal do Rio Grande do
Norte Natal-RN

Jussier Oliveira Vitoriano

DDS, Department of Materials Engineering,
Universidade Federal do Rio Grande do
Norte Natal-RN

Hugo Alexandre de Oliveira Rocha

PhD, Department of Biochemistry, Universidade
Federal do Rio Grande do Norte Natal-RN

Moacir Fernandes de Queiroz Neto

MSc, Department of Biochemistry, Universidade
Federal do Rio Grande do Norte Natal-RN

José Sandro Pereira da Silva

PhD, Department of Dentistry, Universidade
Federal do Rio Grande do Norte
Natal-RN

sputter cage was used for titanium surfaces to improve their biocompatibility with human tissue.

Materials & Methods: The investigation of the biological response of this nitrided surface when in contact with cells with osteogenic potential is essential when you want to use this process in the manufacture of implants. Thus were evaluated in vitro the initial phenomena that culminate in osseointegration of implants, the main adhesion, proliferation and production of alkaline phosphatase from cells of the dental pulp focus. The physicochemical characterization of the surface of TiN was carried out by X-ray diffractometer, atomic force microscopy and wettability tests for determining the static contact angle. **Results:** Cell adhesion was enhanced by surface treatment plasma cathode cage being significantly greater adhesion on the surfaces nitrided TiCN compared with the plate surface.

Conclusions: Moreover, deposition of collagen fibers with production of alkaline phosphatase allows us to infer that there was a differentiation of cells of the dental pulp source in osteoblastic cells.

KEYWORDS: Alkaline phosphatase, Dental pulp, Plasma nitriding, Stem cells, Sputtering cage.

ABSTRACT: Introduction In this study a new method for plasma nitrided called discharge

1 | INTRODUCTION

Since the 60s, when the discovery of osseointegration phenomenon by Swedish doctor Branemark, materials science has been active in seeking a biocompatible material with the biological fluid that allows the complete rehabilitation of the individual. For this purpose, commercially pure titanium (cpTi) and its alloys have proven the materials of choice for forming contact with the air a thin oxide layer (TiO_2), biocompatible with human tissue and reduces the corrosion phenomenon material, besides influencing cell adhesion to the implant surface which is essential for osseointegration of implants. However, the TiO_2 film has vacancies that in contact with the environment are easily filled with contaminants that interfere with cell adhesion (ANSELME, 2000; TAVARES et al., 2009).

Cell adhesion and the consequent proliferation and differentiation in the titanium surface occur by the expression of molecules of the extracellular matrix and transmembrane molecules that bind to specific sites of macromolecules adsorbed on the surface according to the topographical features that these feature (MARTIN et al., 1995; DELIGIANNU et al., 2001). In particular the phenomena of surface energy, wettability and surface roughness that can be modified by the surface treatments that seek to perfecting mechanical features of titanium with surface properties desired to interface with biological phenomena. Among the surface modification processes we can mention the changes by anodizing electrochemical, ion implantation and plasma treatments, among others (KAWAI et al., 2004; CHIANG et al., 2009).

The nitriding technique of plasma sputtering cage allows the deposition of thin and uniform films on various substrates through the effect of hollow cathode, which occurs in the holes of a metal cage, with which are produced titanium compounds by plasma interaction surface of holes being subsequently deposited in an electrically insulated substrate (ALVES et al., 2003). This technique is considered an environmentally clean technique does not cause damage to the environment and a cool technique for allowing the surface treatment at low temperatures, in view of the high temperatures change the homogeneity of surface (MARANDA e NOWAKOWSK, 2006). The thermochemical treatment by plasma cathodic cage allows the formation of TiN_x films (nitridation), TiN_xO_y (oxidonitretação) and TiN_xC_y (carbonitretação) depending on the plasma atmosphere of the variation by the variation of flow of various gases such as $\text{Ar} + \text{N}_2 + \text{H}_2$ and $\text{Ar} + \text{N}_2 + \text{CH}_4 + \text{N}_2 + \text{Ar}$ and O_2 , respectively. The insertion nitrogen ions on the surface allows the formation of a titanium nitride film (TiN_x) with high anti-corrosive and biocompatible potential.

From the insertion of implants in the surgical bed a cascade of biochemical and molecular events is initiated and culminate in the differentiation of undifferentiated mesenchymal cells into osteoblasts that will synthesize the collagen matrix precursor of bone tissue. Undifferentiated mesenchymal cells (MSCs - mesenchymal stem cells) is a stem cell sub-group whose origin sites raise numerous research and its function

is related to the repair processes and tissue healing (HUANG et al., 2009). They differ primarily of embryonic stem cells (ESCs - embryonic stem cells) for these come from embryos with the possibility of differentiation in hundreds of cell types, but which, however, have a high potential for transformation into teratomas and its use promotes numerous ethical conflicts and religious (GRONTHOS, et al., 2002). The MSCs, however, are pluripotent and have less restrictive factors in their research with equal potential to give rise to osteogenic cells, chondrogenic, adipogenic, myogenic, neurogenic, among others and the knowledge gained from its development profile parameter is compared to adult stem cells found in other tissues and organs such as adipose tissue, cord blood, liver, brain, and enamel organ (HUANG et al., 2009).

Recently, the development and dental growth have been associated with adult stem cells and the isolation of these cells in the pulp tissues (DPSCs), periodontal ligament (PDLSCs), apical papilla (SCAPs), dental follicle (DFPCs) and exfoliated deciduous teeth (SHED) was demonstrated. The DPSCs (dental pulp stem cells), forming heterogeneous colonies with different sizes and cell morphology, capacity for self-renewal (9), proliferative potential and differentiation (HARADA e OHSHIMA, 2004). Furthermore, they demonstrated in vivo the formation of dentinogênico material and therefore suggest the possibility of recovering the dental tissues, correction palate, periodontal structures and perhaps a complete replacement of a tooth, and as the extrapolation to use these autologous cells in the formation of hybrid biomaterials and tissue recovery at high potential to differentiate in vitro in different tissues (WADDINGTON et al., 2009).

The aim of this study was to evaluate the influence of titanium nitride film deposited on titanium surface by plasma nitriding in cathodic cage behavior of undifferentiated mesenchymal cells from dental pulp.

2 | METODOLOGY

2.1 Samples Surface Treatment Protocol

Samples of commercially pure titanium type II (cpTi II) com 19mm diameter and 1.5 mm thick initially passed by metallography process in sanding and polishing of silicon carbide colloidal silica and hydrogen peroxide solution. Cleaning was performed with enzymatic detergent RiozymeBive neutral gold diluted to 5% (v \ v) distilled water, sequentially in ultrasound for 10 minutes for each solution. The samples were divided into two groups, the positive control group consisting of polished samples and the experimental group comprised of samples submitted to the processing plasma in a hermetically sealed chamber, where an anode at the top and a polarized cathodically base, upon which it was placed an alumina disc to isolate the sample and over this titanium disks were placed. Around the disks was placed in a cathodic cage and the overlying cover this. Initially, a vacuum was made in the reactor to a pressure

of 0.008 mbar and was introduced hydrogen with a flow rate of 12sccm as a carrier gas of impurities to a 0,2mbar pressure, current of 0.10 milliamp (mA) and 914V, constant temperature of 200 ° C for 20 minutes. Next, nitrogen (N₂) was introduced to 3sccm atmosphere until a stable work around 0,865mbar, 0.38 mA, 831V and 450C temperature. The temperature was monitored by a thermocouple chromium-aluminum-contact with the sample port and controlled by continuously varying the voltage and current between the electrodes. Under these conditions of constant pressure and temperature, the samples were nitrided for 60 minutes and the plasma atmospheres% H₈₀ N₂₀% following a gas flow 15sccm was monitored by mass spectroscopy. Then the samples were sterilized by gamma ray at the Institute of Weights and Measures (IPEN) in the state of Pernambuco in a total 25 kGy of radiation released in average doses of 8,9KGy / h.

2.2 TiN Film Analysis

The positive control group (n = 3) and the experimental group (n = 3) were analyzed by atomic force microscopy, carried out in the Center for Studies in Oil and Natural Gas (NEPGN) / UFRN and testing wettability by determining the static contact angle of the sessile drop technique or by a goniometer developed in Materials Processing Laboratory Plasma UFRN. Water and glycerol were used to obtain the polar and dispersive components, respectively, and determining the surface tension. They were analyzed with the software Pinnacle Studio QuickStart version 8, with the acquisition of photographic images after 60s drop deposition. The mean and standard deviation were performed in SurfTens program and are shown in Table 1. A sample of the positive control group and a sample of the experimental group were analyzed by the diffractometer X-ray in a configuration with incidence beam 5° (five degrees), radiation CuK λ and scan angles between 30 and 80°, steps from 0 02 and a time of 0.6 seconds per step at a rate of 2 / min. The phase identification was made based on existing chips crystallographic literature for metal alloys.

2.3 Obtaining cell groups

Two human teeth of the third molars group, which would be discarded after surgery from a 32-year-old patient, male, were used for obtaining the undifferentiated mesenchymal cells in the coronary and radicular pulp after extraction atraumatic with careful surgical protocol, using conventional surgical techniques and following the rigorous aseptic techniques. The patient was made aware of the importance of research and its acquiescence was established by signing the Consent and Informed (ICF), previously approved by the Research Ethics Committee of the Federal University of Rio Grande do Norte (UFRN) to conform with operational criteria of the National Research Ethics Commission.

Access to the pulp chamber occurred complete odontosecção the crown and root, followed by removal of the coronary pulp by instrumental Lucas and instrumentation of

the root canal with K No. 15 file, to remove the root pulp formed respectively, DPCSs-C groups (dental pulp stem cells coronary) and DPCSs-R (dental pulp stem cells root). Both groups were immersed in falcon tube with α -MEM and transported aseptically ice for Biotechnology Laboratory of Natural Polymers (Biopol) where they were subjected to enzymatic digestion with 6mg / ml collagenase I (Gibco, USA), and 8mg / ml dispase (Gibco, USA), diluted in 2ml of PBS. The suspension was centrifuged at 1200 rpm for eight minutes and the supernatant removed, allowing the precipitated cells were suspended and cultured in small bottles containing basic medium α -MEM (Cultilab, Brazil) supplemented with 15% fetal bovine serum, FBS (Cultilab, Brazil). The cultures were maintained at 37 ° C in 5% CO₂ until they reached 70-90% confluency, with change of medium every three days. In subculture, the basic medium was removed and the plates then added 2 ml of Trypsin / EDTA (0.25% trypsin containing 1 mM EDTA - Cultilab, Brazil). The cell suspension was placed in conical tube with the same volume of α -MEM supplemented with 15% FBS in order to inactivate the trypsin and centrifuged, and the supernatant removed and the cells resuspended in α -MEM medium. A suspension rate of DPCSs-C groups and DPCSs-R in the third passage they were separated for counting in Neubauer chamber and determination of cell viability.

2.4 Behavior of cell groups DPC Ss-C and D'CSs-R

Cells coronal pulp and root pulp taken from bottles fourth passage were plated in triplicate respecting the count 10³, 2x10³, 4x10³, 6x10³, 8x10³, 1x10⁴, 1,2x10⁴ cells / well in 96 well plates to an accompaniment seven days of cell growth as a function of cell density with change of media every three days. The analysis was performed by quantitative test of metabolic reduction of MTT (3- [4,5-dimethyl-thiazol-2-yl] -2,5-diphenyltetrazolium bromide) Aldrick 98% at a concentration of 1mg / ml of alpha medium MEM without FBS (fetal bovine serum) which results in the production of formazan crystals inside the cells. After 4h, cells were lysed by ethanol BP and the absorbance of release of the crystals was measured on a Biotek ELISA equipment.

2.5 Adhesion and proliferation of cell groups DPS-C and D'CSs-R

A cell density of 6,33x10³ cells / well coming from the coronal pulp and root pulp alone were plated in triplicate for the adhesion assays (7 pass) and cell proliferation (3rd pass). The cpTi II polished was used as a positive control surface and the plate has formed the negative control of the assay, when compared to the titanium surface nitrided by plasma sputtering cage. Cell adhesion was measured 3h after the plating staining method by crystal violet 0.2% in 2% ethanol. After 5min contact with the solution the disks were rinsed with PBS to remove excess reagent and immersed in a lysis solution composed of 50% ethanol and 0.1M sodium citrate, which promoted lysis and subsequent release of absorbed reagent by the cells.

Cell proliferation on the surface of cpTi-polished disc (positive control), cpTi-nitrided (case) and plate (negative control) was measured at 24h, 48h and 72h by MTT

method, following the methodology previously described for analysis of cell behavior. The absorbance in each case was analyzed in Elysa -Epoch Biotek meter when 3ml Half of each sample was distributed in three wells of a 96 well plate in the total number of 9 results for each group analyzed and average results of the analyzes of each group are described in chart 1 and chart 2a, b and c for cell adhesion and proliferation, respectively.

2.6 Differentiation of cell groups DPCSs-C and DPCSs-R

Cell differentiation was assessed by plating in triplicate $6,33 \times 10^3$ cells / well DPCSs-C and DPCSs-R in 12-well plates containing groups: positive control, and negative control case. Initially the cells were plated in MEM- α medium that after 24 hours was replaced with 750 μ l of differentiation medium StemPro® Osteogenesis Differentiation Kit Invitrogen GIBCO at a ratio of 90ml of the base medium, 10ml of additional means and 50mL of Sigma A5955 Antibiotic. The absorbance of the alkaline phosphatase is directly proportional to the enzymatic activity of cell groups and analyzed at 7, 14 and 21 days. The culture media of the wells were removed and added to eppendorf tubes for analysis by the kinetic method of fixed time and measurement end point, as recommended in the kit protocol Alkaline Phosphatase Invitrogen. Absorbance was read in a spectrophotometer DR 5000 Hach and linearity calculations phosphatase, represented in the equation below, they were measured by dividing the test absorbance by standard absorbance multiplied by the calibration factor determined by the method.

The equalization of the data was defined by the product of the division of alkaline phosphatase values for the resulting proteins dosagetotals obtained by the Bradford method based on the color change of Brilliant Coomassie Blue G-250 in a track of 590nm. For the total protein content of an aliquot removed from the test means 7, 14 and 21 days were added to test tubes and diluted with distilled water 1:20. Subsequently, 1 μ l of Bradford reagent at a ratio of 1: 4 with distilled water, was added to the test tube.

For analysis by optical microscopy confocal 4 titanium disks, 2 discs of the positive control group and 2 group disks case were cultured with DPSCs-C and DPSCs-R for 21 days in the middle of osteogenic differentiation and subsequently stained with Picro solution -Sirius Red (Direct Red 80). Initially, the samples were immersed in hematoxylin for 8 min and washed in distilled water until complete removal of excess dye. The Picro-sirius red solution was deposited on the surface of the discs and these were incubated for 60min at room temperature. An acid water solution (5ml of acetic acid in 1 liter of distilled water) was used to wash the samples were then dehydrated in ethanol PA.

2.7 Statistical analysis

Data were analyzed by Anova single factor for identification of variance between groups, p-value <0.1 is considered significant and the analysis by T-Student between

two samples assuming unequal variances between samples when p values <0.05 were considered significant. The correlation between the data analysis was established by Pearson (Pearson's r) where $r = 1$ product showed a direct correlation, $r = -1$ products demonstrated an inverse correlation $r = 0$ it shows that a variable does not depend linearly on another.

3 | RESULTS

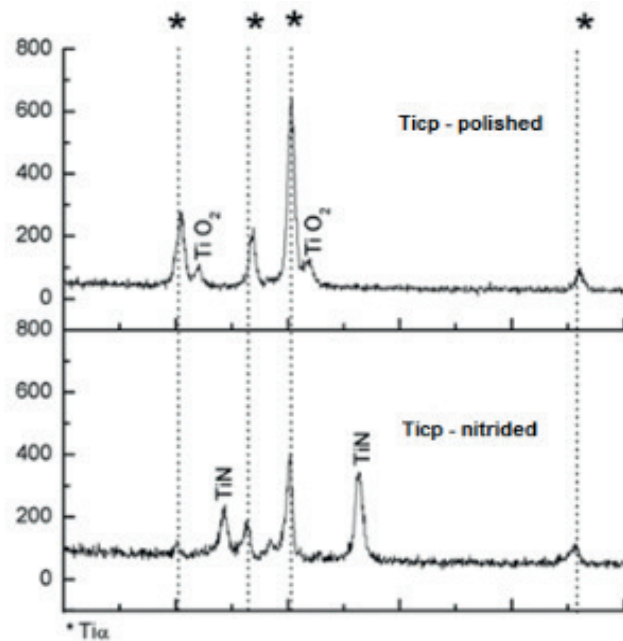


FIGURE 1- TiN film analysis graph diffraction of x-ray.

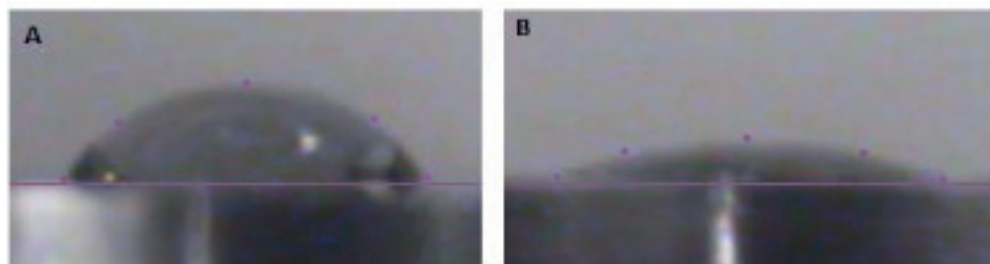


FIGURE 2 - Sensitivity drop technique wettability tests

samples	water	δ	glycerol	δ	γ_s^p	γ_s^d	γ_s
AM1	69,66	0,9	67,75	0,8	23,45815	9,60547	33,06362
AM2	70,05	0,5	68,41	0,5	23,53790	9,22243	32,76033
AM3	69,48	0,9	70,28	0,7	26,90032	6,74517	33,64549
AM4	19,35	0,96	19,97	0,61	54,01254	15,30871	69,32124
AM5	15,68	1,04	20,55	0,53	57,65684	13,61463	71,27146
AM6	18,83	0,94	23,22	0,67	56,84814	13,28163	70,12977

TABEL 1 - Wettability values and surface energy.

Ticppolished	Ticpnitrided
--------------	--------------

	AM 1*	AM 2*	AM 3*	AM 4*	AM 5*	AM 6*
Ra	0,9990	0,7730	1,2110	11,6860	12,6730	10,1710
Rz	29,1370	21,6790	21,4960	142,4170	120,8480	97,2060
Rzjis	12,3500	8,0260	7,5970	60,7110	54,2120	43,7270
Rq	1,4790	1,1290	1,5660	14,7630	15,7820	12,6040
Rp	24,1520	15,2430	15,9500	85,3210	65,5980	50,2010
Rv	4,9850	6,4360	5,5460	57,0960	55,2490	47,0050

TABEL 2 - Roughness analysis table by AFM. * lengthX 5.00[um]/lengthY 5.00 [um]/surface 25.000 [(um)2]/values in [nm]. AM - samples.

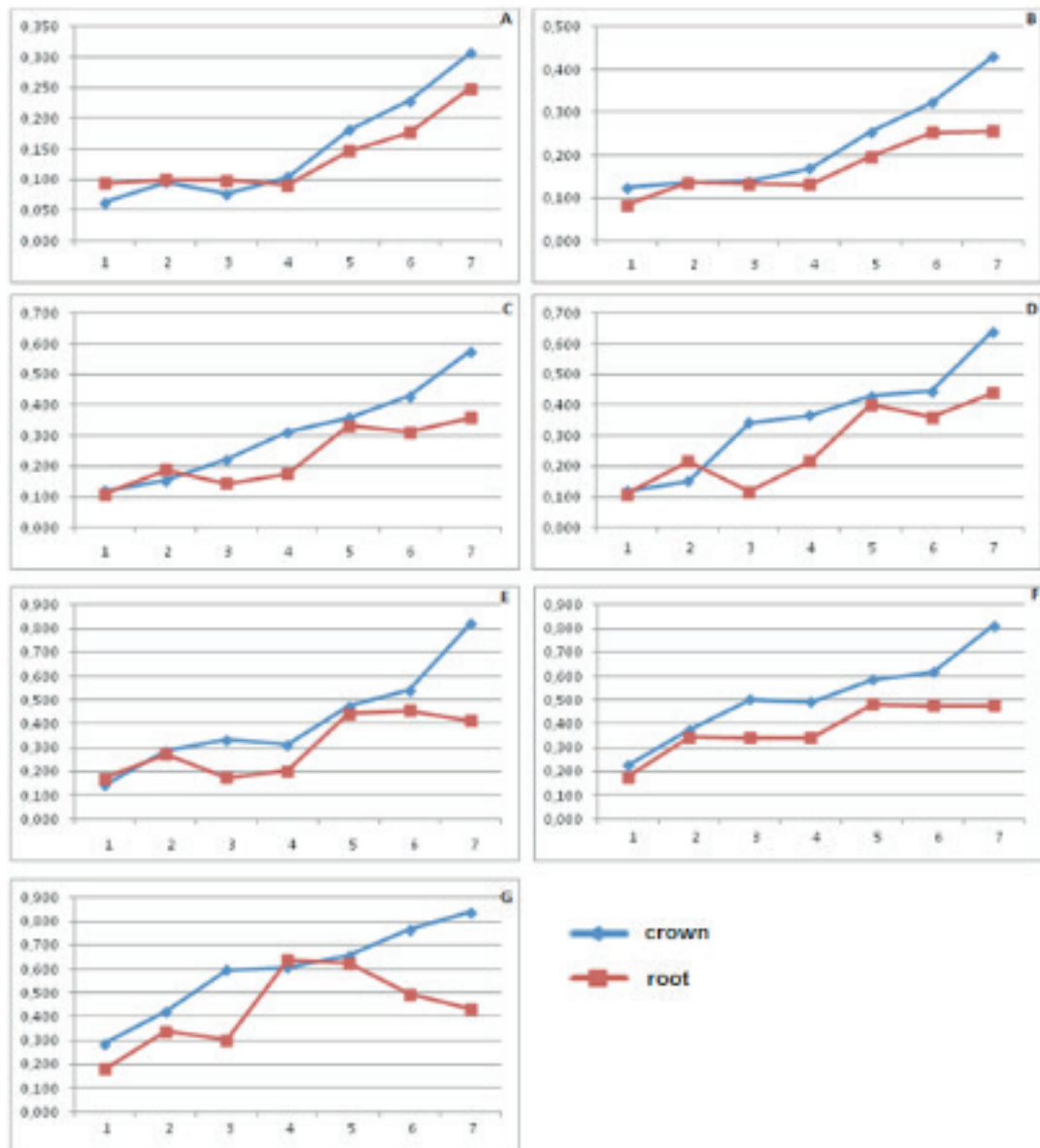


FIGURE 3 - Cellular behavior analysis charts. The cell density = 103 B = cell density of 2x103. C = cell density of 4x103. D = cell density of 6x103. E = cell density of 8x103. F = cell density of 104 G = 1,2x104 cell density.

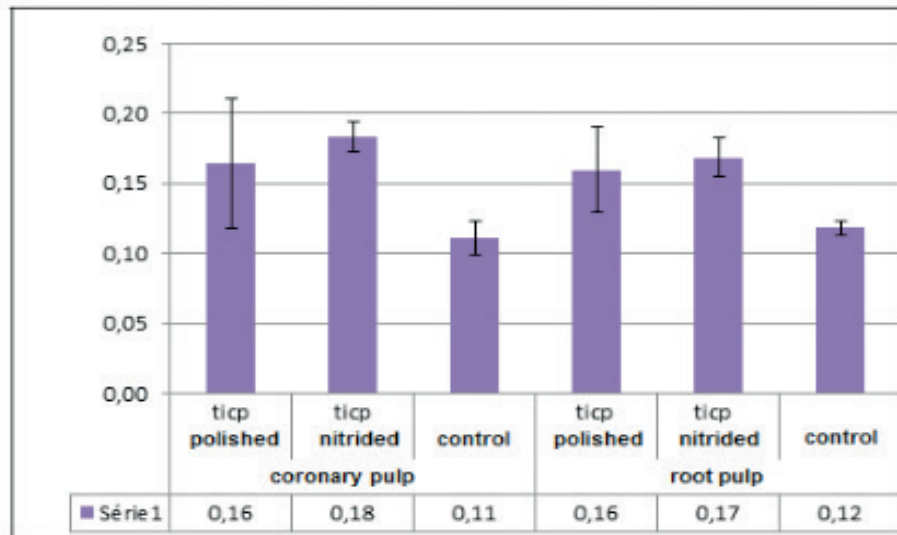


FIGURE 4- Graph of cell adhesion after 3h plating.

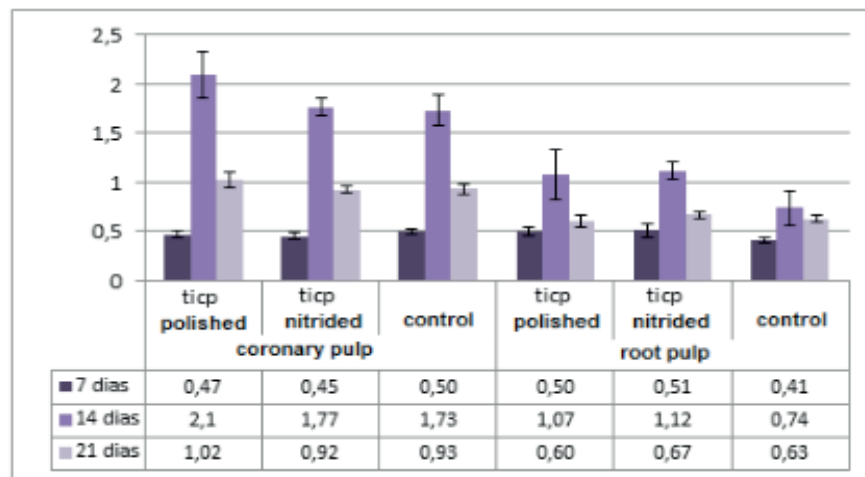


FIGURE 5- Graph of cell proliferation.

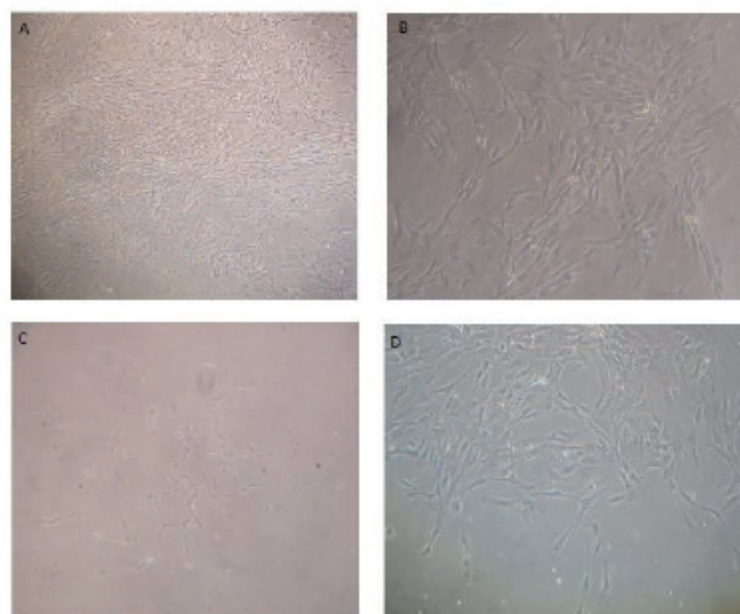


FIGURE 6 - Optical microscopy of DPSCs-C (A and B) and DPSCs-R (C and D). Magnification 100x (A and C) and 500X (B and D)

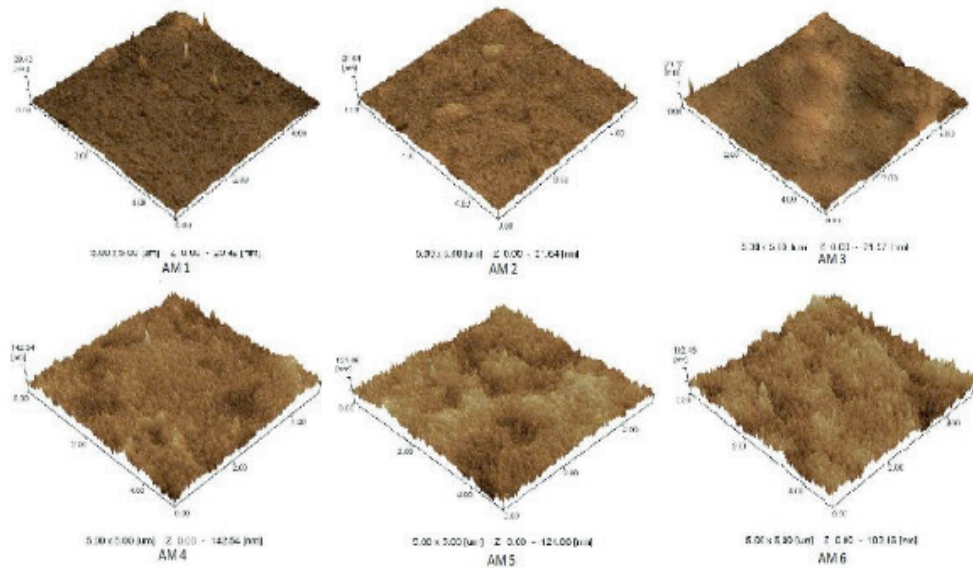


FIGURE 7 - AFM analysis of polished titanium surfaces (AM 1; AM2; AM3) and plasma nitrided titanium surfaces (AM4; AM5; AM6).

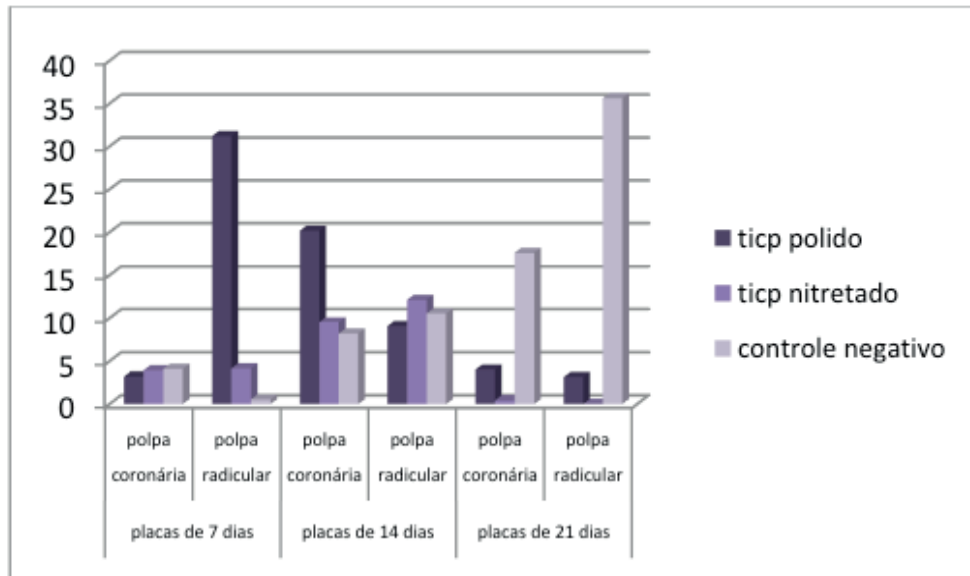


FIGURE 8 - Osteogenic Differentiation Potential

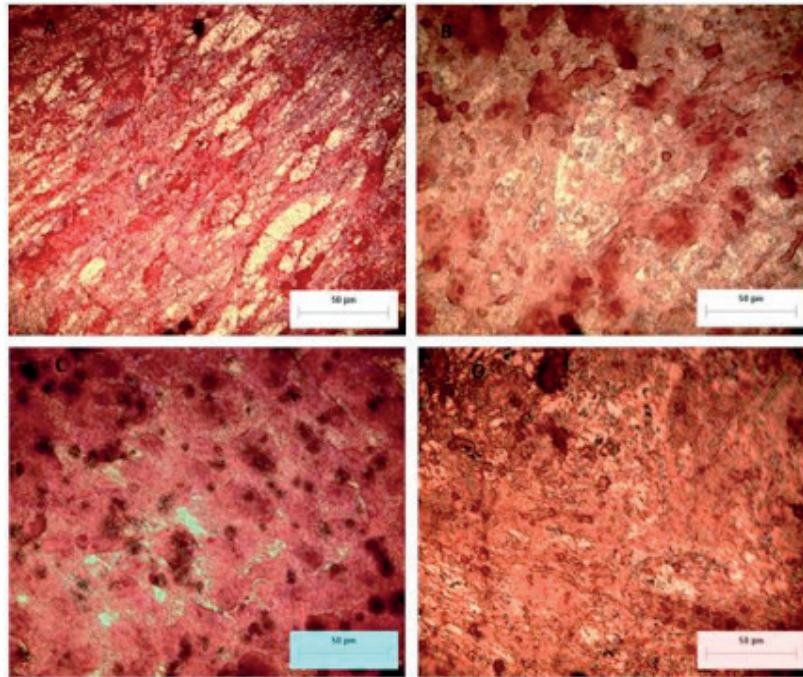


FIGURE 9. Optical microscopy of picocircius red staining 21 days after plating. A- cpTi polished DPSCs II-C; B- cpTi II nitrided DPSCs-C; C cpTi polished DPSCs II-R; D-II cpTinitrided DPSCs-R.

4 | DISCUSSION

The enamel organ development is determined by the interaction between the mesenchymal oral tissue and ectodermal cells derived from the neural crest, which can interfere in the characteristics of DPSCs (KAWAI et al., 2004; TAVARES et al., 2009). Himunoistoquímico studies and RT-PCR showed the mesenchymal DPSCs the expression of stro-1 factor and positive vimentin, and the cells with LANGFR markers indicative of embryonic neural cells additionally expressed the CD105 and Notch 2 markers which confirm the presence of different strains of stem cells in the pulp dentária. However, research with DPSCs is still quite immature and questioned even if the stem cells were present in the pulp tissue or would come from the vascular circulation (ALVES et al., 2003; MARANDA e NOWAKOWSKI, 2006).

The coronal pulp originates from the dental papilla, while the root pulp comes from the apical papilla, soft tissue located at the apex of the permanent teeth developing and from which the SCAPs, which could highlight the differences and similarities found between coronary DPSCs and root in vitro. The origin of this difference can be related to the continuous development of the apical papilla for root formation, necessitating cells more undifferentiated potential, while the cells in the coronal pulp would act only as stockers post-injúria odontoblasts in the process of formation of reparadora dentin (MARANDA e NOWAKOWSKI, 2006) . In response to stimulation of osteogenic cells apical papilla (SCAPs) expressing CD24 which has not been found in BMSCs or DPSCs. Stem cells have the potential of adipogenic differentiation, chondrogenic and osteogenic were isolated from the roots of two incisors indicating the endodontic

treatment four days after trauma and automobile compared to stromal cells exfoliated deciduous teeth. PCR reactions were performed to identify stem cell markers and differentiation markers. The two sources of cells demonstrated the presence of stem cell markers and differentiation capacity similar to BMSCs (presence of CD29 markers, CD90 and CD105), however, exhibited reduced expression of CD14, CD34 and CD45, which are markers specific for cells hematopoietic stem (DELIGIANNI et al., 2001; KAWAI et al., 2004). This work shows the presence of stem cells in the root pulp, and the possibility of extrapolation of obtaining stem cells, and the third molars indicating extraction and primary teeth to permanent teeth that have experienced trauma, without bumping into ethical factors can contradict the procedimento (HARADA e OSHIMA et al., 2004).

The DPSCs human cultures were investigated for their viability and cell vitality, morphology, cell adhesion and proliferation, mineralization capacity, as well as the interference imposed on these characteristics by the difference of location between coronary and root pulp. The research was conducted by inverted microscopy for analysis of cell morphology and by the use of commercial kits for the detection of the formation of mineralized foci. The research results demonstrated the presence of multipotent cells in both pulp tissues, especially the above results and better characteristics in radicular pulp tissue (HUANG et al., 2009).

In this study cell viability demonstrated in the count results in a Neubauer chamber, represented by values of $10,9 \times 10^6$ and $4,79 \times 10^6$ in the case of coronary cells and root cells, respectively, reflects a rapidly developing coronary forward cells to pulp cells roots which have grown about two times less and visually showed a sparse spread over the bottle, while the coronal pulp cells expanded on the entire surface (fig. 3 and 6). However, coronary and radicular pulp cells have a similar initial proliferation (Fig. 3) with the exception of the concentration of $1,2 \times 10^4$ in which cells derived from the coronal pulp had a significantly higher growth compared to cells of the radicular pulp evidenced by average results 0.2863, 0.1803 and a standard deviation of 0.0366 and 0.005, respectively. This behavior, which was repeated throughout the experiment and leads us to realize a higher development of coronary cells with cells of the root pulp and which is accentuated when in higher densities (fig.6). Furthermore, the cells of the radicular pulp had a proliferation with cell death (Fig.3) or plateau formation around the second and 4th days and again rising generally around the 3rd and 5th days. Coincidentally, these events occur synchronously to the period established for the exchange of culture medium and indicate a higher adjustment of coronary cells continue to proliferate linearly and more homogeneous regardless of the decrease of nutrients in the medium or the cell density.

The deposition of TiN films increases the biocompatibility of the titanium substrate by raising anti-corrosive effects of metal in contact with biological fluids. The bombardment of the surface with nitrogen ions enabled the formation of TiN_x in the analyzed samples and reduction of TiO_2 and $\text{Ti}\alpha$ peaks, as seen in Fig.1. The film

formed modified surface topography and roughness changed as shown by average values Ra of 0.994 \pm 0.22 and \pm 1.26 \pm 11.510 for samples nitrided and polished cpTi (tab -2), respectively and $p = 0.0004$ (t-student test) demonstrating a significant difference in values roughness. The Ra values are commonly used for indicating the average values of the variation of the peaks and valleys from the mean line of the imaginary surface profile. These values give us a partial analysis of the topography, and its completion can be obtained by dividing the value of Rp, the peak value analysis by Rz, the average roughness obtained in five unit meas. The product of this equation allows us to evaluate the topography of the surfaces showing the outline of peaks present, while the samples of polished cpTi II had an average value of 1.33 and samples nitridedcpTi II showed a mean value of 1.82, both of \pm 0.01 and $p = 0.082$ (student's t test), showing that there is a significant difference in the topography of the samples by the formation of more pronounced peaks on the surface of the nitrided samples, as well shown in the fig. 7.

The topographical and chemical properties of surfaces of materials determine the protein adsorption on the surface and thus determine the cellular interactions with the biomaterial. The cell adhesion phenomenon is determined by an initial, immediate phase of water adsorption on the surface followed by deposition of intrinsic proteins of the extracellular matrix and the quality of the primary phenomenon for the development of cell attachment stage involving physico-chemical bonds and strength Vander Waals ionic strengths, as well as cell adhesion phase itself that occurs in the long term by the expression of cell membrane proteins, especially the integrins family proteins and influence the morphology, cell proliferation and differentiation (ANSELME, 2000).

The variation in surface roughness increases the surface area available for cell attachment changing the proliferation, differentiation and production of extracellular matrix by determining the phenotypic expression of osteoblastic cells this factor is extensively associated with the tissue response in vitro and in vivo however, there is disagreement on the choice of the roughness with osteoblastic cells genotype, although it recognized its potential to distinguish different roughness of surfaces and different topographies similar roughness (HUANG, 2005).

The ANOVA analysis of cell adhesion data after three hours shows that there is variance between the adhesion of cell groups of coronary pulp cpTi polished, nitridedcpTi and negative control with $p = 0.06$ and the root pulp groups with values $p = 0.01$. Following statistical analysis by t-student difference was found between the samples nitridedcpTi and the negative control group showed average of 0.18 and 0.11, respectively and $p = 0.0004$ between cells coronal pulp and 0.17 and 0.12 respectively and $p = 0.01$ between cells of the radicular pulp, demonstrating that the nitrided surface altered cell adhesion when compared with the plastic surface which constituted the negative control group.

In this analysis there was no significant difference in cell adhesion between the polished cpTi groups and nitretatocpTi of both cell groups as reported by the values of $p = 0.59$ and $p = 0.61$ (t-student) to DPSCs-R and DPSCs C, respectively, however,

the Pearson correlation analysis with $r = 1$, Ra as compared values and the average of cell adhesion DPSCs-C and DPSCs-R, has demonstrated a positive correlation between the roughening and cell adhesion phenomenon in both cell groups. Regarding the pattern of cell adhesion intra cellular groups there was no difference between DPSCs-C and DPSCs-R with values of $p = 0.89$, 0.22 and 0.20 for groups of polished cpTi, nitridedcpTi and negative control respectively. Moreover, it remained cell behavior pattern (Fig. 4), since the cells of the coronal pulp and root pulp cells showed a similar initial adhesion in all groups.

Cell proliferation showed a negative correlation $r = -1$ in the case of DPSCs-C is a positive correlation $r = 1$ to DPSCs-R as a function of Ra on 7, 14 and 21 days. This demonstrates that the proliferation of the cells underwent coronary pulp influence of other phenomena besides roughness, since DPSCs-C showed a positive correlation with respect to Ra for the cell adhesion phenomenon which is the trigger of cell proliferation. The average values of the proliferation of negative control of both cell groups show that the behavior of cells in 7, 14 and 21 days maintained the pattern established in the cellular behavior analysis (Fig.5) with greater adaptation of DPSCs-C in relation to DPSCs-R and by decreased proliferation as a function of time can be attributed to adverse factors of cell density saturation and reduction of nutrients in the medium. Although the initial values of cell proliferation in seven days suggest that contact with the polished and nitridedcpTi a reversal of this cell behavior being the most adapted DPSCs-R that DPSCs-C, a continuous analysis of proliferation in 14 days reports growth about 4.5x the DPSCs-C-R DPSCs while only doubling the proliferation values .

The wettability expressed by the materials is their hydrophilicity and water molecules inserted into the blood tissue are those which first hit the surface, and this factor correlated to the adsorption of proteins on the surface and consequently the cell adhesion (Fig. 7). The deposition of TiN film substantially alter the hydrophilicity of the surface (Fig. 2) with decrease of the average contact angle polished cpTi of 69.73 to 17.95 on the surface of nitridedcpTi $p = 0.0005$ (t -Student).

The influence of roughness on the surface of hydrophilicity is widely researched and there is no consensus on the interference of this phenomenon in wetting angles, and some authors even suggest an adaptation of Yung angle by inserting a correction factor concerning the roughness. What we see in this test was a negative correlation between Ra and wettability with $r = -1$, showing that the change of surface roughness by the deposition of the TiN film maintains an inverse relationship to the wetting angle and a directly proportional relationship $r = 1$ em relationship the polar and dispersive components as well as the surface tension for assessing biomaterial surface energy (Tab 1 and 2) which is influenced by roughness and topography of the surface (Fig. 7) (DELIGIANNI et al., 2001; TAVARES et al., 2009).

The change in surface energy changes the cell deposition on the surface and commonly osteoblastic cells prefer to adhere to biomaterials that exhibit a 60dinas

surface energy, however, the tests conducted here did not allow this correlation given that there was no difference Cell adhesion between the polished surfaces nitrided and cpTicpTi, as discussed above (DELIGIANNI et al., 2001).

The alkaline phosphatase is a protein released by cells during pre-osteoblastic cell differentiation process which usually occurs between 7 and 14 days for mesenchymal stem cells. The differentiation potential has been established by the product of the alkaline phosphatase, total protein demonstrates that the total number of viable cells in the differentiation process. The of fig. 8 data enables us to measure the DPSCs-C cells and DPSCs-R cultured in the negative control, maintained a continuous differentiation in the three periods analyzed and a maximum peak differentiation after 21 days, whereas the cells cultured polished cpTi showed an peak differentiation for 7 days for the DPSCs-R with subsequent decrease in the other periods, and a maximum peak at 14 days for DPSCs-C and both cultured cell groups cpTinitrided peaked alkaline phosphatase for 14 days.

The DPSCs-R cells showed rapid adaptation to cpTi surface differentiating into osteoblasts at 7 days with a significant difference of cell differentiation potential between the polished cpTi and negative control, as well as between the nitridedcpTi and control negative and polished and nitridedcpTicpTi. However, an individual analysis by t-student alkaline phosphatase values of DPSCs-R (Fig. 8) does not assume difference between polished and cpTicpTinitrided, $p = 0.78$, demonstrating that the differentiation potential was amended by range total protein. The student t-analysis between the values of alkaline phosphatase cpTi of nitrided DPSCs-C to 7 days, also shows a significant difference, $p = 0.03$, for the DPSCs-C cpTi polished, and the film formation TiN favoring the differentiation of mesenchymal cells.

While the potential of cell differentiation at 14 days indicates a marked differentiation of DPSCs-C polished cpTi t-student alkaline phosphatase test between the polished cpTi and cpTinitrided surfaces do not show differences $p = 0,76$, but demonstrates a difference between the polished surfaces nitrided and cpTicpTi, $p = 0.04$, for DPSCs-R being nitrided surface favorable to the development of this cell group (Fig. 8).

The osteoblast cells deposit a collagen matrix which will subsequently be mineralized giving rise to bone tissue. The collagen fibers deposited on all surfaces demonstrate the biocompatibility of the polished surface cpTi II and II cpTinitrided to allow the functional expression of the cells. These data associated with the production of alkaline phosphatase demonstrates the differentiation of the undifferentiated mesenchymal cells.

The picosirius stain red stains collagen fibers allowing to evaluate the hue and the spatial arrangement of fibers, and the orange color allows distinguishing thicker collagen fibers, regarding the arrangement of DPSCs-C fibers in II polished surface of cpTi., which also showed an array organized fibers as compared with DPSCs-C TicpIlnitrided groups (Fig. 9) DPSCs-R and polished TicpII DPSCs-R cpTinitrided (RICH e WHITTAKER, 2005).

5 | CONCLUSIONS

- The viability and proliferation assays show a greater adaptation of the coronary pulp cells compared to cells of the root pulp.
- Cell adhesion is favored by plasma surface treatment cathodic cage being significantly greater adhesion on the surfaces of nitridedcpTi compared with the negative control surface.
- The difference in cell adhesion cpTi polished surfaces nitrided and cpTi was not significant, although there is a positive correlation between increased roughness and cell adhesion.
- The nitrided surface by cathodic cage promotes osteoblastic differentiation of coronary and radicular DPSCs, anticipating that period compared to the negative control.
- The plasma nitrided surface favored differentiation DPSCs-C in seven days when compared to the polished surface and favored cell differentiation in 14 days for DPSC-R.
- The deposition of collagen fibers associated with the production of alkaline phosphatase allows us to infer that there was a differentiation of mesenchymal stem cells into osteoblast cells.

REFERENCES

ALVES JR. C., HAJEK V., DOS SANTOS C.A. **Thermal behavior of supersolidus bronze powder compacts during heating by hollow cathode discharge.** Materials Science and Engineering: A. 2003 5/15;348(1-2):84-9.

ANSELME K. **Osteoblast adhesion on biomaterials.** Biomaterials. 2000 4//;21(7):667-81.

CHIANG C-Y, CHIOU S-H, YANG W-E, HSU M-L, YUNG M-C, TSAI M-L, et al. **Formation of TiO₂ nano-network on titanium surface increases the human cell growth.** Dental Materials. 2009;25(8):1022-9.

DELIGIANNI DD, KATSALA N, LADAS S, SOTIROPOULOU D, AMEDEE J, MISSIRLIS YF. **Effect of surface roughness of the titanium alloy Ti-6Al-4V on human bone marrow cell response and on protein adsorption.** Biomaterials. 2001;22(11):1241-51.

GRONTHOS S., BRAHIM J., LI W., FISHER L.W., CHERMAN N., BOYDE A. et al. **Stem cell properties of human dental pulp stem cells.** J Dent Res. 2002 Aug;81(8):531-5. PubMed PMID: 12147742. Epub 2002/07/31. eng.

HARADA H., OHSHIMA H. **New perspectives on tooth development and the dental stem cell niche.** Arch Histol Cytol. 2004 Mar;67(1):1-11. PubMed PMID: 15125018. Epub 2004/05/06. eng.

HUANG G.T., GRONTHOS S., SHI S. **Mesenchymal stem cells derived from dental tissues vs. those from other sources: their biology and role in regenerative medicine.** J Dent Res. 2009 Sep;88(9):792-806. PubMed PMID: 19767575. Pubmed Central PMCID: Pmc2830488. Epub 2009/09/22. eng.

HUANG H-H, HSU C-H, PAN S-J, HE J-L, CHEN C-C, LEE T-L. **Corrosion and cell adhesion behavior of TiN-coated and ion-nitrided titanium for dental applications.** Applied Surface Science. 2005 5/15;244(1-4):252-6.

KAWAI H., SHIBATA Y., MIYAZAKI T. **Glow discharge plasma pretreatment enhances osteoclast differentiation and survival on titanium plates.** *Biomaterials*. 2004 5//;25(10):1805-11.

MARANDA-NIEDBAŁA A, NOWAKOWSKI R. **AFM of titanium nitride layers prepared under glow discharge conditions.** *Journal of Alloys and Compounds*. 2006 11/9//;424(1-2):272-8.

MARTIN J.Y, SCHWARTZ Z., HUMMERT T.W., SCHRAUB D.M., SIMPSON J., LANKFORD J, JR., et al. **Effect of titanium surface roughness on proliferation, differentiation, and** *J Biomed Mater Res*. 1995 Mar;29(3):389-401. PubMed PMID: 7542245. Epub 1995/03/01. eng.

RICH L., WHITTAKER P. **Collagen and picosirius red staining: a polarized light assessment of fibrillar hue and spatial distribution.** *Braz. J. morphol. Sci.* 2005. p. 97-104.

TAVARES J.C.M, CORNÉLIO D.A., DA SILVA N.B., BEZERRA DE MOURA C.E., DE QUEIROZ J.D.F., SÁ J.C., et al. **Effect of titanium surface modified by plasma energy source on genotoxic response in vitro.** *Toxicology*. 2009 8/3//;262(2):138-45.

WADDINGTON R.J., YOUDE S.J., LEE C.P., SLOAN A.J. **Isolation of distinct progenitor stem cell populations from dental pulp.** *Cells Tissues Organs*. 2009;189(1-4):268-74. PubMed PMID: 18701814. Epub 2008/08/15. eng.

SOBRE O ORGANIZADOR

Henrique Ajuz Holzmann: Professor da Universidade Tecnológica Federal do Paraná (UTFPR). Graduação em Tecnologia em Fabricação Mecânica e Engenharia Mecânica pela Universidade Tecnológica Federal do Paraná. Mestre em Engenharia de Produção pela Universidade Tecnológica Federal do Paraná. Doutorando em Engenharia e Ciência dos Materiais pela Universidade Estadual de Ponta Grossa. Trabalha com os temas: Revestimentos resistentes a corrosão, Soldagem e Caracterização de revestimentos soldados.

ÍNDICE REMISSIVO

A

Alumina-zircônia 154, 156

Aptasensor 51, 52, 54, 55, 56, 57, 58, 60, 87, 88, 91, 92, 93

Área específica 108, 115, 116, 117, 142, 143

B

Biogás 23, 24, 25, 26, 27, 28, 29, 31, 32, 33, 34, 35

Biomateriais 74, 75, 209

C

CdTe/CdSe 161, 162, 163, 164, 165, 168, 169, 170

Compósito 1, 2, 3, 4, 5, 6, 7, 8, 10, 13, 15, 16, 17, 18, 19, 20, 21

Conversão 108, 110, 112, 115, 116, 118

E

Eletrofiação 73, 74, 75, 77, 79, 80, 81, 83, 119, 122, 123, 124, 125, 126, 131

Eletroquímica 52, 53, 55, 57, 60, 63, 64, 65, 66, 67, 68, 87, 88, 89, 91, 92, 189

Engenharia tecidual 74

Espaçamento de fibra 1

F

Fase Anatase 133, 135, 136, 140, 141, 142, 143

Fator de Qualidade 146, 147, 151, 152

Fibra de Juta 10, 12, 22

Fibra de vidro 10, 12, 13, 20, 21

Fibras de carbono 36, 37, 38, 40, 49

Fibras de sisal 1, 2, 3, 7, 14

Fibras naturais 1, 2, 10, 11, 12, 13, 21

Filtro 23, 28, 33, 97

Fosfato metálico 133

Fotocatálise 133, 134, 135, 142, 144

G

Gelatina 108, 110, 111

Genossensores 64, 65, 66

H

H₂S 23, 24, 25, 28, 29, 32, 33, 34

Híbrido 10, 13, 21

I

Indutores Internos 146, 151

L

Laminados 8, 10, 11, 12, 13, 14, 15, 16, 18, 19, 20, 21

LaNiO₃ 119, 120, 121, 123, 124, 125, 126, 127, 128, 129, 131

M

Meniscos 73, 74, 75, 80, 81, 83

Microdomínios 36, 38, 40, 44, 45, 46, 47, 48, 49

N

Nanocompósito 96, 99, 101, 104, 105

Nanocristais 162

Nanopartículas de Ouro 63, 66, 68

Nanotubo de carbono 51, 87

Neuroesquistossomose 63, 64, 65, 70, 71, 72

Núcleo/casca 162

O

Ocratoxina A 51, 52, 87, 88

Óxido de zinco 51, 52, 54, 87, 89, 90, 96, 97, 98, 99, 100, 101, 103, 104, 106, 205, 206

P

Pechini 23, 24, 27, 34, 108, 109, 110, 111, 118

Perovskita 108, 109, 110, 111, 112, 113, 114, 116, 117, 120

Piche mesofásico 36, 38, 40, 41, 42, 43, 44, 45, 48, 49

Poli(ácido láctico) 96, 97

Propriedades mecânicas 1, 2, 5, 10, 12, 13, 21, 36, 37, 38, 49, 75, 83, 97, 98, 104, 106, 154, 155, 156, 158, 159, 209

R

Rádio Frequência 146, 147

S

Síntese coloidal 162

Sol-Gel 122, 132, 133, 134, 136, 144

T

Teoria mesoscópica do contínuo 36, 39

U

Umidade 12, 14, 23, 24, 25, 27, 28, 31, 32, 33, 52, 77, 97, 123, 137, 230, 239, 240, 241

